Available online at www.sciencedirect.com

ScienceDirect

Advances in Space Research 71 (2023) 199–215

ADVANCES IN SPACE RESEARCH
(a COSPAR publication)

www.elsevier.com/locate/asr

The day-to-day variability in the mesosphere and lower thermosphere in low latitudes: A study using MF radar

H.P. Gaikwad [a,b], S. Fadnavis [c], O.B. Gurav [d], J.L. Bhosale [a], A.K. Sharma [e,*], P.T. Patil [f], R.N. Ghodpage [f], M.M. Sutar [a], G.A. Chavan [g], A.T. Birajdar [a], D.J. Shetti [h]

[a] *Department of Physics, Shikshanmaharshi Dr. Bapuji Salunkhe College, Miraj, MS 416410, India*
[b] *Department of Physics, Kisan Veer Mahavidyalaya, Wai, MS 412803, India*
[c] *Centre for Climate Change Research, Indian Institute of Tropical Meteorology, Pune 411008, India*
[d] *Department of Physics, Bharati Vidyapeeth (Deeemed to be University), Yashwantrao Mohite College of Arts, Science and Commerce, Pune, MS 411038, India*
[e] *School of Physics, Shri Mata Vaishno Devi University, Kakryal, Katra, Jammu & Kashmir 182320, India*
[f] *MF Radar, Indian Institute of Geomagnetism, Shivaji University Campus, Vidyanagar, Kolhapur, MS 416004, India*
[g] *Department of Physics, Sir Parashurambhau College, Pune 411030, India*
[h] *Department of Physics, Smt Kasturbai Walchand College, Sangli, MS 416416, India*

Received 19 March 2022; received in revised form 12 August 2022; accepted 24 August 2022
Available online 28 August 2022

Abstract

This study presents the analysis of planetary waves (PWs) using daily mean wind velocities for four years (August 2013 to July 2017) of continuous measurements using MF radar over the low latitude Indian region Kolhapur (16.8° N; 74.2° E). The MF radar at Kolhapur was upgraded in 2013. These are the first results of PWs after the upgradation of MF radar. The seasonal and intra-seasonal variabilities of East-West (EW) traveling PWs in the MLT region have been studied. In the present work, the data was analyzed to study the waves with various periodicities (e.g. 3–4, 5–8, 15–17, and 30–60 days). The 3.5 day [Ultra-Fast Kelvin (UFK)] wave shows semiannual variability with burst like wave activity observed during the summer months and December solstice. In addition, it is observed to be stronger in the spring equinoctial period. A strong semiannual oscillation (SAO) has been observed in a 6.5-day wave with peaks near the equinoxes. Similar to SAO over the low latitude MLT region, the wave activity is stronger in April/May than in September/October. The 6.5-day waves are observed to be stronger when the background mean wind is westward. From the analysis, it has been seen that the period before and after the equinoctial period is favorable for the 6.5-day wave propagation. The 16-day wave has no significant seasonal dependence; instead, the waves spread to almost all seasons. The Madden-Julian Oscillations (MJOs) have been observed to be propagating with an average wind speed of $\sim$ 5 m/s when the background mean wind is eastward. The occurrence of MJO is observed during the summer and winter months. These results are the first of their kind in two aspects: first, they show the PWs with enhanced altitude coverage covering up to 110 km, and second, they show the PWs not contaminated due to equatorial electro jet influence.

Keywords: Mesosphere and Lower Thermosphere; Planetary waves; Low latitude; MF radar

* Corresponding author.
E-mail addresses: herambgaikwad01@gmail.com (H.P. Gaikwad), suvarna@tropmet.res.in (S. Fadnavis), omgurav91@gmail.com (O.B. Gurav), bhosalejl@gmail.com (J.L. Bhosale), ashok.kumar@smvdu.ac.in (A.K. Sharma), ptpiigkop@yahoo.com (P.T. Patil), rupeshghodpage@gmail.com (R.N. Ghodpage), smilind20066@gmail.com (M.M. Sutar), gangadharchavan2@gmail.com (G.A. Chavan), appu.birajdar12@gmail.com (A.T. Birajdar), jitushetti@gmail.com (D.J. Shetti).

https://doi.org/10.1016/j.asr.2022.08.066

1. Introduction

The presence of global scale disturbances superimposed on circumpolar westerly winds is one of the most noticeable features in the winter stratosphere of the Northern Hemisphere (NH). The disturbances seem to be stationary in nature (i.e., fixed to the Earth). It has been thought that these disturbances are dynamically coupled with those in the troposphere and are associated with the surface condition of the Earth (Matsuno, 1966; Reed, 1965, 1964; Reed et al., 1963). These waves propagate upwards and transport momentum and energy to the higher altitudes. As these waves propagate to higher altitudes, their amplitude grows, and at the same time, the waves are dispersed by mechanical (Rayleigh) friction and other radiative processes. The breakdown of the wave takes place as it grows in amplitude, which generates turbulence (Vincent, 1984). The wave is dissipated, momentum deposited and accelerates background atmosphere (Reddi and Ramkumar, 1995). The planetary scale oscillations are of two types. The westerly propagating Kelvin waves and easterly Rossby waves in the lower stratosphere give rise to alternatively westerly and easterly regimes, respectively (Holton and Lindzen, 1972).

The Kelvin waves are equatorially trapped, which transports the momentum towards the east in the middle atmosphere. These waves are forced by latent heat release in the form of large-scale convective clusters in the tropical troposphere. In the absence of mean wind shear, these Kelvin waves are supposed to have a Gaussian structure with maximum amplitudes at the equator in the zonal wind, vertical velocity, pressure, and temperature. And the amplitude decays exponentially with latitude. Again, Kelvin waves are broadly classified into distinct frequency bands as slow, fast, and ultra-fast Kelvin (UFK) waves. These waves are characterized on the basis of periodicity. The slow Kelvin waves have periods of 10–20 days with a phase speed of 20–40 m/s and a vertical wavelength of 10 km and were first observed by radiosonde balloon in the lower stratosphere (Wallace and Kousky, 1968). The slow Kelvin waves are characterised by wavenumber 1 having an eastward phase velocity of 20–40 m/s and a vertical wavelength of 10 km. The Kelvin waves are eastward propagating zonal wavenumber 1 with a period of 10 days and a vertical wavelength of 20 km. These waves have a phase speed of 50–80 m/s and are observed in the upper stratosphere with rocketsondes (Hirota, 1978; Hitchman and Leovy, 1988). The existence of ultrafast Kelvin waves is confirmed by satellite remote sensing measurements with a zonal phase speed exceeding 100 m/s and a 3–4 day wave period (Garcia et al., 2005; Guharay et al., 2011; Lieberman and Riggin, 1997; Salby et al., 1984; Sridharan et al., 2002).

The Rossby waves are westward propagating waves and generally have discrete periodicities between 4 and 20 days. For example, 5–8 days are referred to as 6.5-days, and 15–17 days are referred to as 16-days. Theoretical studies on the influence of non-uniform background wind fields on normal mode structures and periods of Rossby waves have been made using numerical models. The 6.5 day wave is a Rossby wave with zonal wave number 1 ($s = 1$) (Liu et al., 2004; Talaat et al., 2001; Talaat and Yee, 2002; Yee et al., 2001) having a vertical wavelength of roughly 50–80 km (Talaat et al., 2001; Talaat and Yee, 2002) and propagating vertically with decreasing phase with height (Yee et al., 2001). The 16-day wave is westward propagating with zonal wavenumber (Forbes et al., 1995; Luo et al., 2002 & references therein), maximum amplitude is found at above 80 km (Jiang et al., 2005; Namboothiri et al., 2002; Shankar, 2012 & references therein) and vertical wavelength is observed to be 30–50 km (Shankar, 2012). Eastward motion of background wind is favorable for 16-day wave propagation to MLT regions (Das et al., 2010; Jiang et al., 2005; Namboothiri et al., 2002). (Salby M., 1981) presented a detailed calculation for various modes up to the upper mesosphere. He reported that the influence of the non-uniform wind field on the modes is very large, with relatively slow travelling velocities. This activity is observed in solstice conditions as spatial non-uniformities of the zonal mean wind field are very large in the stratosphere and mesosphere heights, so the 6.5- and 16-day waves are confined to the winter stratosphere and mesosphere.

A remarkable feature of the tropical atmospheric circulation and moist convection is their tendency to be organized at planetary scales. These oscillations propagate eastward at an average speed of 5 m/s across the equatorial Indian and western/central Pacific oceans. The period of these oscillations is 30–90 days. The phenomenon shown in Fig. 1 is known as the Madden-Julian Oscillation (MJO). The MJO has been much studied since it was discovered by Madden and Julian in 1971. The MJO is observed in zonal wind and causes rainfall over the Indian Ocean and western and central Pacific. The MJO in the zonal wind is out of phase in the lower and upper troposphere. The MJO can be considered to be a mixture of Kelvin and Rossby waves near the source region and propagates eastward away from it (Zhang, 2005).

The 3.5-day ultra-fast Kelvin wave in the mesopause region is extensively studied using MF radar at Tirunelveli (8.7° N; 77.8° E), India by S Sridharan et al., (2002). They reported the semiannual variability at ~ 85 km where the Mesopause Semiannual Oscillation (MSAO) in the mean wind peaks. Also, they qualitatively showed that the mean eastward winds and their shears are associated with a burst of waves with moderate amplitude. Takahashi et al., (2006), studied the signature of 3–6 day equatorial planetary waves in the mesosphere and ionosphere. They have utilized meteor radar measurements of MLT winds at Cariri (7.4° S, 36.5° W) and Ascension Island (7.9° S, 14.4° W), as well as the minimum ionospheric virtual height, h′F, measured at Fortaleza (3.9° S, 38.4° W) in 2004. They reported that the 3.5 and 6.5-day waves could propagate upward from the stratosphere to the MLT and could interact with the ionosphere, modulating the F-region dynamo

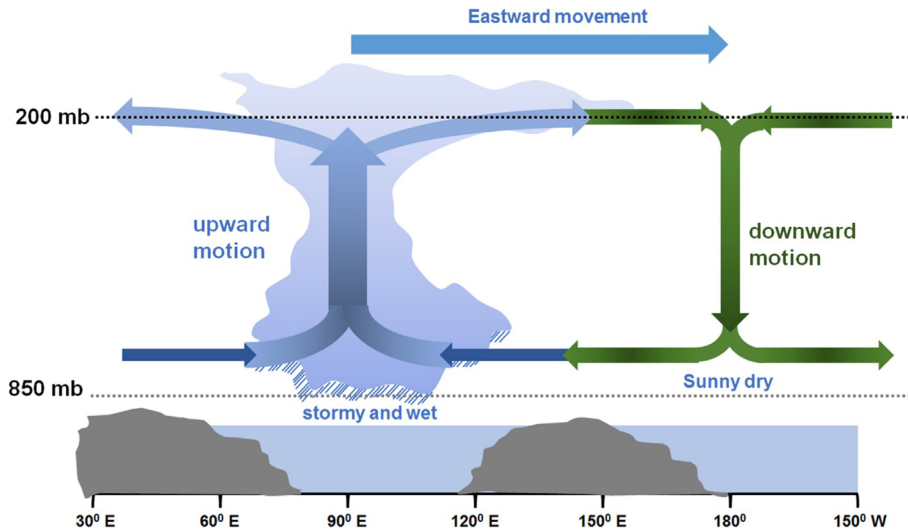

Fig. 1. The surface and upper-atmosphere structure of the MJO (Zhang 2005).

and E-region conductivity. Takahashi et al., (2007) studied the UFK waves from Cariri and Fortaleza and TIMED/SABER satellite temperature data of the stratosphere-mesosphere. They have reported the first clear evidence of the propagation of a UFK wave from the stratosphere to the ionosphere, and there could have been an important role of UFK waves in the day-to-day variability of the equatorial ionosphere evening uplift. Talaat et al., (2001) reported an observational study of 6.5-day Rossby waves and concluded from the seasonal and spatial analysis that these waves are modified by the zonal mean wind. They have also observed the vertical structure of the 6.5-day wave, which indicates that it is an internal gravity wave. Talaat and Yee, (2002) reported from the tropical station that the westward propagating 6.5-day wave is prominent during the equinox. The 6.5-day wave was extensively studied by Kishore et al., (2004) using MF radar at Tirunelveli. They found the 6.5-day wave to be stronger in the zonal component, equinoctial phenomena, and the possible effect of SAO on this wave. The seasonal variability of the 6.5-day wave in the middle and upper atmosphere was studied by Liu et al. (2004). For this, they used thermosphere-iono sphere-mesosphere-electrodynamics general circulation model (TIME-GCM) data. They have reported that the wave amplitudes during equinoxes are smaller than the peaks before and after, but are still larger than those during solstices. This is because of baroclinic/barotropic instability; such instability is usually absent during equinoxes. Jiang et al. (2008) studied the mesospheric 6.5-day wave observed by the radar system at various locations: Platteville (40.18° N, 104.7° W), Yamagawa (31.2° N, 130.6° E), Tirunelveli (8.67° N, 77.82° E), and Adelaide (35° S, 138° E). They examined the relationship between the 6.5-day wave and the background wind and concluded that the background wind does not significantly affect the vertical propagation of the 6.5-day waves because of its faster phase speed (~65 m/s). (Forbes et al., 1995; Luo et al., 2000) investigated the quasi-16 day Rossby wave in MLT using radars in Obninsk, Russia (54° N, 38° E) and Saskatoon, Canada (52° N, 107° W). They performed numerical simulations which confirmed the interpretation that this resulted in direct upward penetration of the disturbance and which provided the corresponding global wind fields, geopotential heights, and temperatures. Luo et al., (2000) reported seasonal variation in wave characteristics (vertical wavelength) of quasi 16-day oscillations in the MLT region over Saskatoon and the effect of background wind on the wave. The 16-day planetary waves were studied using multi-MF radar observations from the Arctic to the Equator performed by Luo et al. (2002). They compared their results with HRDI measurements and the GSWM modelling results. They found at mid- and high-latitude locations that the 16-day waves are usually pervasive in the winter-centered seasons (October through March), with the amplitude gradually decreasing with height. Furthermore, the waves are no longer confined to the subtropical and equatorial regions; they have spread to almost all seasons in the MLT region. Ramkumar et al. (2006) conducted an observational study to investigate the effects of the tropical lower atmosphere ~ 20-day oscillations on the ionospheric electrojet. They have used the MST radar, Rayleigh Nd-Yag lidar Gadanki (13.5° N, 79.2° E) and MF radar data at Tirunelveli. They have reported on the basis of observational evidence that long-period oscillations near 21- and 30-days generated in the lower atmosphere (troposphere and lower stratosphere) in the Indian tropical regions have possible influences on the lower E region ionospheric currents (equatorial electrojet [EEJ]) at these periodicities. Luo et al. (2001) also reported that an extra-long period (20–40 day) oscillation is generally observed during the winter (November–March) atmosphere and strong amplitudes are observed throughout the mesosphere.

In the present study, the day to day variabilities in the MLT waves are reported using MF radar wind observations operated at low latitude station Kolhapur (16.8° N;

74.2° E) India with higher altitude coverage covering up to 110 km. From this MF radar data, we report the characteristics of the observed UFK, 6.5-, 16- day waves and MJOs in the MLT region at this location. We show that the UFK waves undergo semi-annual variability in the mesopause region where MSAO is dominant in the mean zonal wind. In addition to this, large intraseasonal variability in MJO, semi-annual variability in 6.5-day wave is also reported. Further, we have discussed the reason for the 16- day wave penetration into the MLT region.

2. Data and methodology

The wind data used in this study were collected using the spaced antenna mode of the MF radar at Kolhapur. The system and mode of operation and the method of wind determination are the same as described by (Vincent and Lesicar 1991). The MF radar system at Kolhapur was upgraded in 2013. The altitude coverage has been enhanced from 98 km to 110 km in upgradation. As we know, at E region height, the MF radar returns would most likely be from total reflections. As a result, we anticipate that these returns will be much stronger than weak partial reflections from the D region. The magnitude of these returns would be reduced by each ground reflation and by any D region absorption during each transition, but the return may still be strong enough to contaminate weak returns from region D even after multiple reflections. During the day, there is a very strong absorption in the D region. As a consequence of this, the typical E region height peaks at 110 km during daytime (Reid, 2015). Thus, additional information covering higher altitudes (E region rather than non-contaminated D region) from this radar can be beneficial to understand the dynamics of this low latitude MLT region. The system details and important results on mean winds and Quasi Two Day Waves observed over Kolhapur are reported earlier by Sharma et al. (2018) and Gaikwad et al. (2019) respectively. The MF radar measurements can provide valuable information in understanding the origin of the field aligned currents and are influenced by electrodynamical processes in the equatorial E region (Dhanya et al., 2008; Gurubaran et al., 2007; Gurubaran and Rajaram, 2000; Ramkumar et al., 2002). The results of previous work (Sharma et al., 2018) using this site clearly revealed the MF radar echoes at 90 km and above are not influenced by electrodynamical processes (Briggs, 1977). To study the long-term oscillations over Kolhapur, the daily mean MLT wind velocities for the observational period from August 2013 to July 2017 are considered. The days having more than 18 data points (18 h of data) are considered for the analysis and the daily mean is calculated for those days only. Linear interpolation is applied to fill the gaps in the time series. There are no noticeable data gaps observed during the period of observations. To study the wave characteristics, various analysis techniques like Fast Fourier Transform (FFT), wavelet analysis, time domain filtering, harmonic analysis, etc. are used, which will be discussed later in the results and discussion section. These results might be useful to understand the planetary scale oscillations over the low latitude MLT region.

2.1. Spectral analysis using FFT technique

To investigate the long-period oscillations present in observed MLT zonal and meridional winds, the daily mean data is subjected to FFT. This technique is capable of yielding the temporal variability in the wave energy. Fig. 2 (a) and (b) depict the FFT of the day mean zonal and meridional winds through contours, respectively. These contours are for the period between 2 and 110 days. The oscillations below 20-days are presented by line plots (shown in Fig. 3). The zonal wind contour (Fig. 2 (a)) clearly shows that the amplitude is maximum/peak near 60–65 and 70–75 days at an altitude of 80–94 km. In addition to this, the peaks are observed at lower thermospheric heights (above 100 km) as well, but their amplitude is observed to be less than mesospheric heights. These features of planetary waves are observed and reported for the first time with this radar from this location. It has also been observed that the oscillations have a period of ~ 48 days. In contour, for merid-

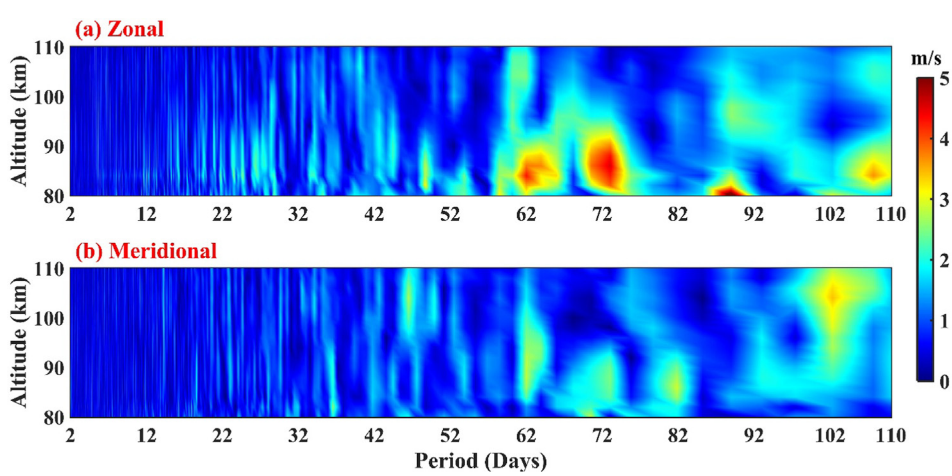

Fig. 2. Amplitude spectra of the mean (a) zonal and (b) meridional wind.

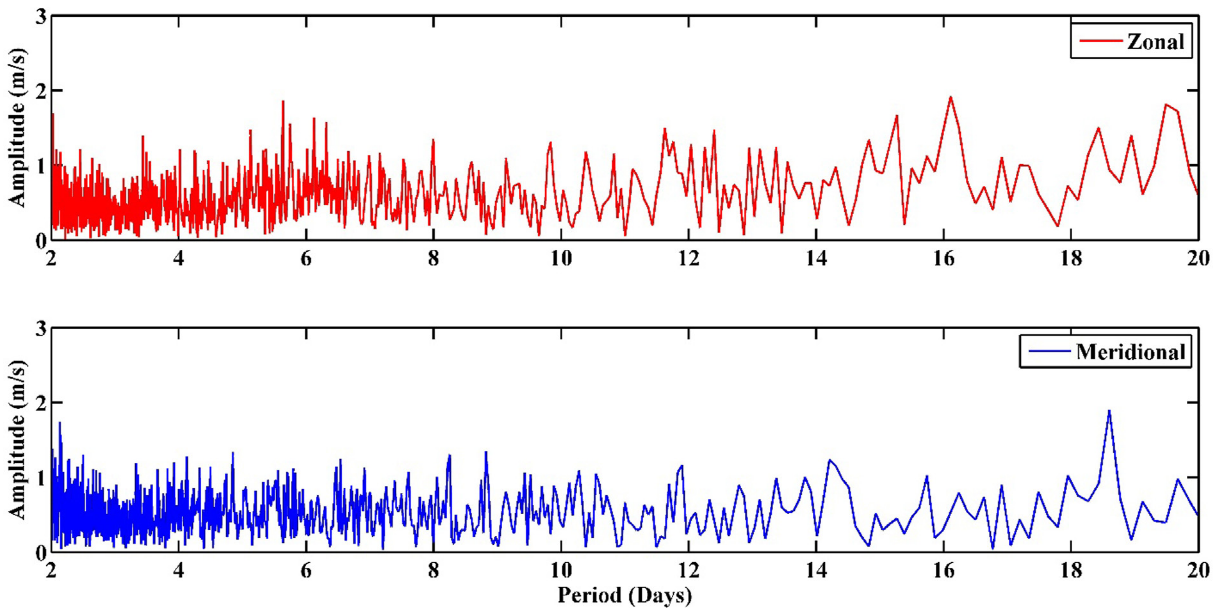

Fig. 3. Amplitude spectra of daily mean zonal and meridional winds at 88 km for the year 2013–2016.

ional wind (Fig. 2 (b)), the oscillations above 40-days are clearly seen. Also, the oscillations near 60–65 and 70–75 day periods are present but with less amplitude as compared with the zonal component.

The line plot of FFT spectra for the zonal and meridional wind is shown in Fig. 3. For a clear view of the oscillations having a period below 20 days, Fig. 3 has been presented separately. The dominant period oscillations are clearly seen in the zonal as well as meridional components. In the zonal wind, the peaks observed at 3.5-, 6.5-, and 16-day correspond to 3–4, 5–8, and 15–17 day oscillations. In the case of meridional wind, the peaks are observed at 3.5-, 6.5-, and 16-day, which corresponds to 3–4, 5–8, and 15–17 day oscillations. Generally, the meridional wind has a smaller amplitude than the zonal wind. These planetary scale waves are discussed in later sub-sections.

2.2. Harmonic analysis

To determine the amplitude and phase of the planetary waves (PWs), the daily average wind data was harmonically analyzed using a time series constructed from hourly mean values. Time series for zonal and meridional wind components were least square fitted with prevailing and 3.5-, 6.5-, 16-, and 45-day harmonic components. Each wind component can be represented by a time-dependent expression.

$$A(t) = a_0 + \sum_{4}^{m=1} A_m \cos\left(\frac{2\pi t}{T_m} + \varphi_m\right) \quad (1)$$

where a_0 is the prevailing component,$A_m and \varphi_m$ are the amplitude and phase of the mth harmonic component with a period of T_m (Vincent et al., 1998). The results using this analysis technique are later discussed in the subsequent 3.1.3, 3.2.3, 3.3.3 and 3.4.3 sections.

2.3. Wavelet analysis

Planetary waves are usually transient phenomena, meaning the data contains non-stationary power at different frequencies. For time–frequency analysis, wavelet analysis has to be applied. Here, the Morlet wavelet is used (Pancheva et al., 2016; Pancheva and Mukhtarov, 2000; Torrence and Compo, 1998).

The contour of wavelet amplitudes for zonal (EW) wind (height averaged 86–94 km) is shown in Fig. 4. The thick contour encloses regions with a significance level greater than 95 %. The X-axis shows the day number, and the Y-axis shows the time periods of the observed oscillations. The solid line shown in wavelet spectra is the “cone of influence”. From the contour (Fig. 4), it can be seen that the observed peaks of 30–60, 15–17, and 5–8 day oscillations are well above the 95 % confidence level. The 6.5 day wave activity exhibits large inter annual variability, with 2015 being the most active compared to 2014 and 2016. The 16 day wave is observed to be dominant in the winter season throughout the analyzed period and spread over all seasons of the year 2014. The detailed results are discussed in subsequent sections.

2.4. Time domain filtering using band-pass filter

The band-pass filtered signal with an appropriate pass band is then plotted for time-height cross-section with superimposition of line contour of monthly mean winds (Figs. 5, 6, 10, 11, 14, 15 & 18). In line contour, solid lines indicate eastward (northward) and dotted lines indicate westward (southward) flow in zonal (meridional) winds. In colored (filled) contours, positive colors indicate eastward (northward) while negative colors indicate westward (southward) flow in zonal (meridional) winds.

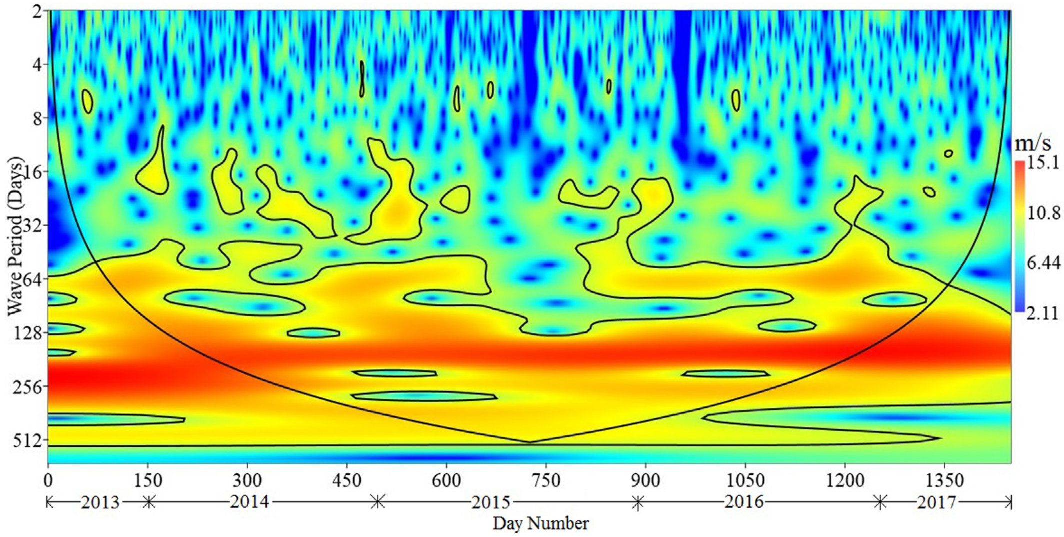

Fig. 4. Wavelet spectra of zonal wind averaged between 86 and 94 km.

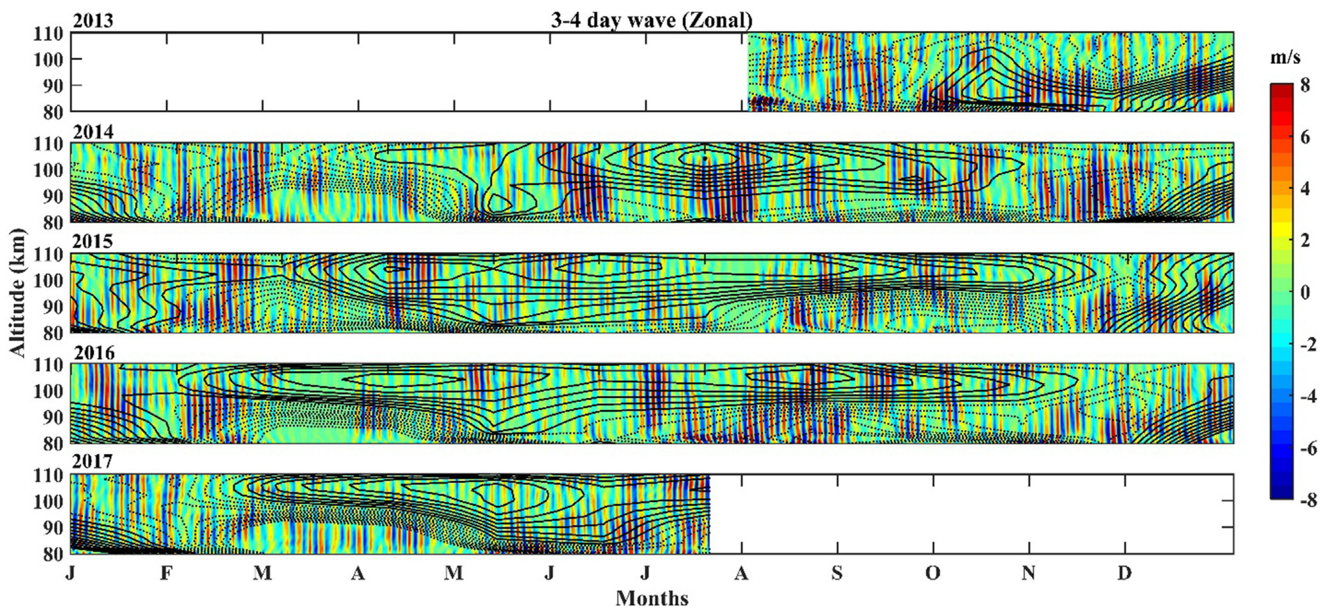

Fig. 5. Contours of 3.5- day band-pass filtered zonal wind superimposed with mean zonal wind from August 2013-July2017 for 80–110 km height.

3. Results

3.1. 3.5 day waves

3.1.1. Time domain filtering

The time-height contours of a band-pass filtered with pass-band were chosen between 3- and 4- days for zonal and meridional winds and are presented in Figs. 5 and 6, respectively. The filtered wave is shown for different years through different contours. And the line contour of the monthly mean background wind is superimposed on it. Overall, ~8 m/s amplitude is observed for a 3.5-day wave. In the 3.5-day filtered zonal wind (Fig. 5), a burst of 3.5-day wave activities are clearly observed in the Northern Hemisphere (NH) summer months (May-August) and during the December solstice period between altitudes of 80 and 100 km, when the background mean wind is eastward. Therefore, these waves can also be referred to as UFK waves. It seems that the wave has an enhancement in the westward shear region during the month of February of every year and also during the fall/autumn equinoctial period (i.e., September-October). The 3.5-day wave activity is at its peak (88–92 km altitude) during November-December and February of all years, March 2017, and April-May 2015 and 2016.

The increase in UFK wave activity observed in 2014, 2015, and 2016 occurred primarily at almost all altitudes above 80 km during the eastward phase of the Mesospheric

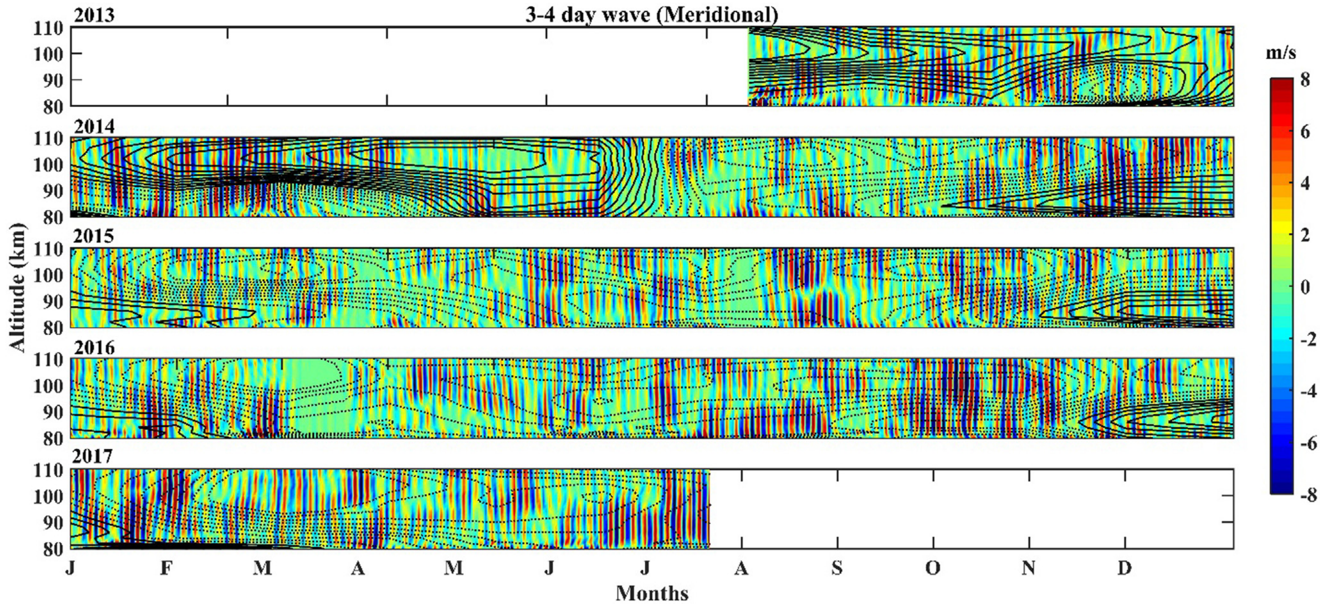

Fig. 6. Contours of 3.5- day band-pass filtered meridional wind superimposed with mean meridional wind from August 2013-July2017 for 80–110 km height.

Annual Oscillation (MAO) (e.g., June and August 2014, April 2015, and July-August 2016) and at times of peak westward flow of background wind (e.g., the intense wave activity observed during the autumn of 2016 and during both westward phases in 2014, 2015, and 2016). This is because of the interaction of the wave with the mean zonal wind field in the underlying stratopause SAO regime (Sridharan et al., 2002; Yoshida et al., 1999). The period of enhancement of UFK wave activity is somewhat similar during all years. The UFK wave activity and the zonal winds in the MLT region were distributed over the whole year during all the analyzed years.

Fig. 6 depicts the 3.5-day filtered meridional wind. There was a bit less than 3.5-day wave activity observed in the meridional wind. From the figure, we can clearly see the 3.5-day wave activity is strong during equinoxes (spring and fall) and summer months when the background mean wind is southward. The amplitude of the wave observed during the equinoctial period is $\sim$ 8 m/s and during the summer months it is $\sim$ 6 m/s. During the summer and fall equinoctial periods, the wave activity is observed at all altitudes (i.e., 80–110 km), while during the spring equinoctial period (March–April), it is between 80 and 100 km. On the one occasion during the December solstice of every year, the wave is enhanced in the northward shear regions. The 3.5-day wave activity is somewhat similar for all the years of both the components (i.e., zonal and meridional).

3.1.2. Seasonal variation in 3.5- day wave

The seasonal variation in 3–4 day wave activity is shown through the analysis of Fig. 7 (time-height cross-section of wave amplitude). The analysis revealed that the zonal wave activity (Fig. 7(a)) is particularly strong during the winter months (November-February), June-July, and March of each year. The peak wave activity (amplitude $\sim$ 6 m/s) is observed at 85–90 km during June-July of every year. At these heights, the Mesopause SAO in zonal wind peaks. It has also been observed that the wave activity is strong when the background wind is eastward. Similar to the zonal component, the meridional (Fig. 7 (b)) 3–4 day wave activity is observed to be strong during winter and summer months.

3.1.3. Amplitude and phase variation of the 3.5-day wave

The amplitude and phase variation of both the components of the 3.5-day wave during the summer and winter months are shown in the analysis of Figs. 8 and 9. The amplitudes are calculated by using harmonic analysis and least square fitted for the 3.5-day harmonic component. It has been observed that the zonal wave amplitude (Fig. 8) is high at all altitudes below 100 km during the summer as well as in the winter months. The wave amplitude below 100 km is observed to be large during the summer months as compared with the winter months. There is no significant phase variation observed during these seasons, and the phase gradually decreases with height. Also, the meridional component shows the wave activity during summer and winter months. From the vertical profile of 3.5-day meridional wave amplitude (Fig. 9), a large inter-annual variability was observed in both seasons. Also, a large phase variation of the wave is observed.

3.2. 6.5 day wave

3.2.1. Time domain filtering

The time-height cross-section of band-pass filtered zonal and meridional winds with pass-band between 5 and 8 days are shown in Figs. 10 and 11 respectively. The filtered wave is shown for different years through different contours. The

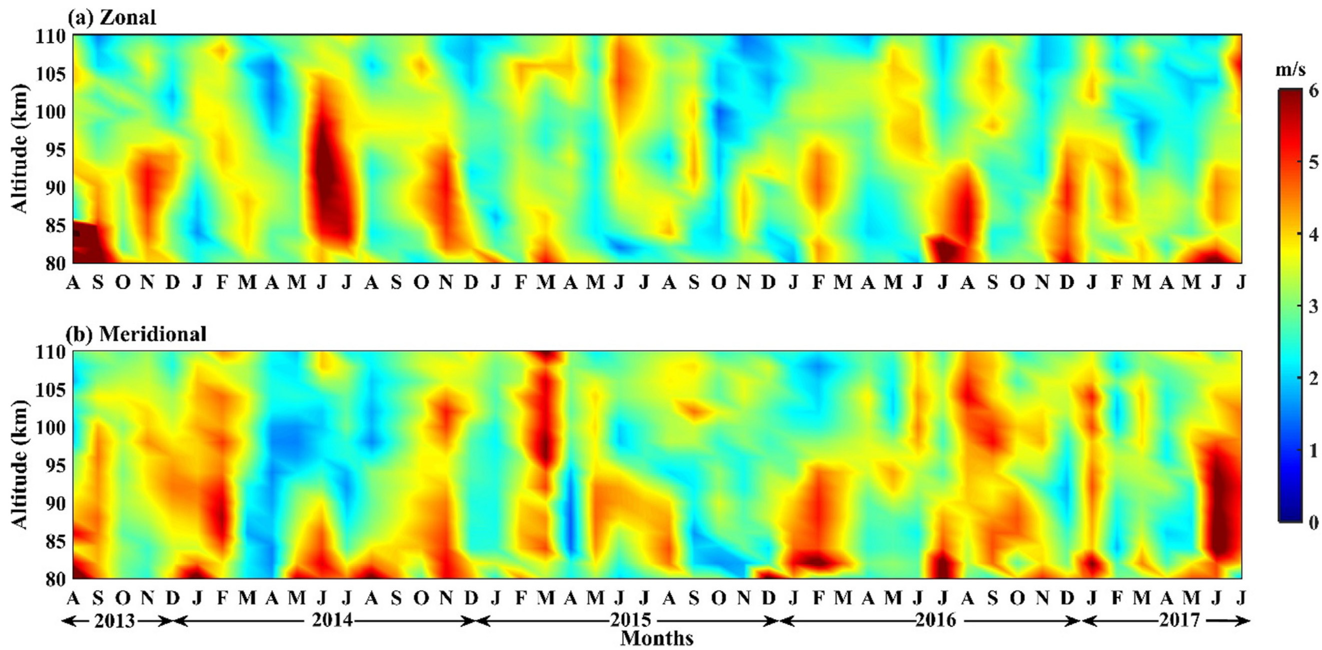

Fig. 7. Seasonal variation in (a) zonal and (b) meridional 3–4 day wave.

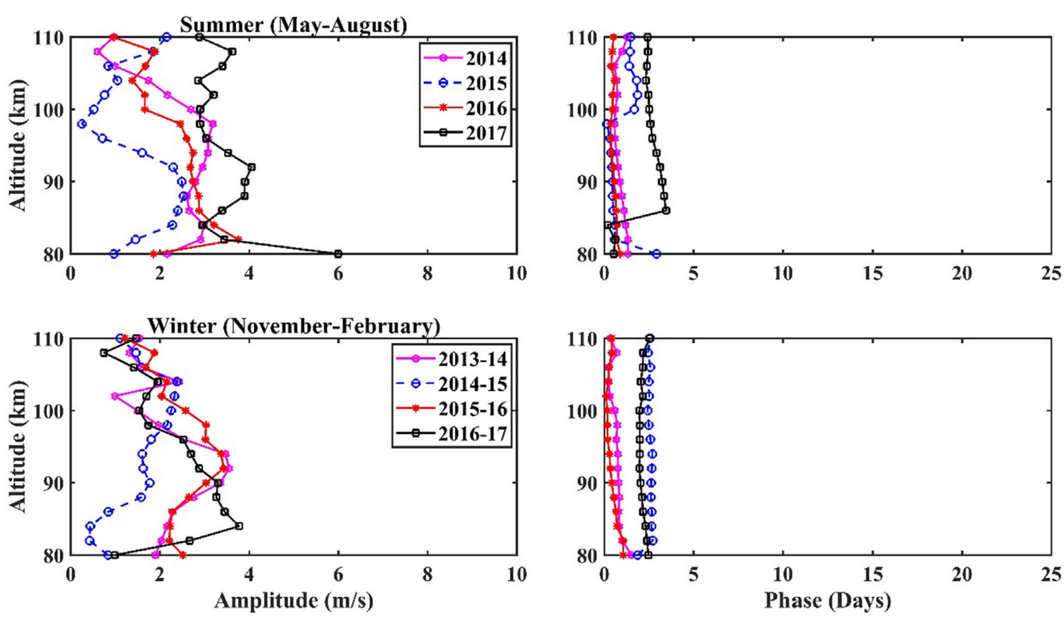

Fig. 8. Vertical profile of the 3.5- day wave amplitude (left panel) and phase (right panel) of zonal wind during summer (upper panel) and winter (lower panel) seasons.

line contour of monthly mean wind is superimposed on these contours of the respective year. The 5–8 day wave is also referred to as 6.5-day wave and it seems to be prominent near equinoxes i.e. April-May and September-October. These waves are westward propagating zonal waves since the background mean wind during the equinoctial period is westward. Similar to the results were reported by (Liu et al. 2004)), the wave amplitudes during equinoxes are smaller than the peaks before and after but are still larger than during solstices. The wind conditions before and after the equinox, are favorable for the wave propagation and amplification. The zonal 6.5-day wave activity (Fig. 10) occurs at all altitudes with a peak amplitude of 10 m/s. The 6.5- day wave activity is observed to be stronger near spring equinox as compared with fall equinox, which is consistent with the results reported earlier by (Kishore et al., 2004). The year 2015 seems to have a peak 6.5- day wave activity than that of 2014 and 2016, since the burst like wave activities was observed during these years. The enhancement in eastward shear regions

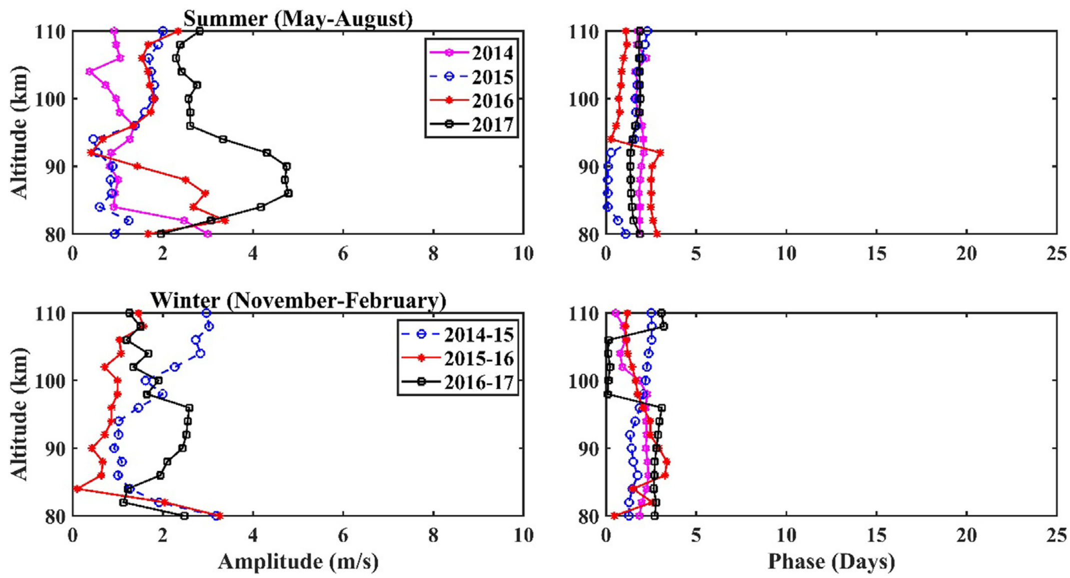

Fig. 9. Vertical profile of the 3.5- day wave amplitude (left panel) and phase (right panel) of meridional wind during summer (upper panel) and winter (lower panel) seasons.

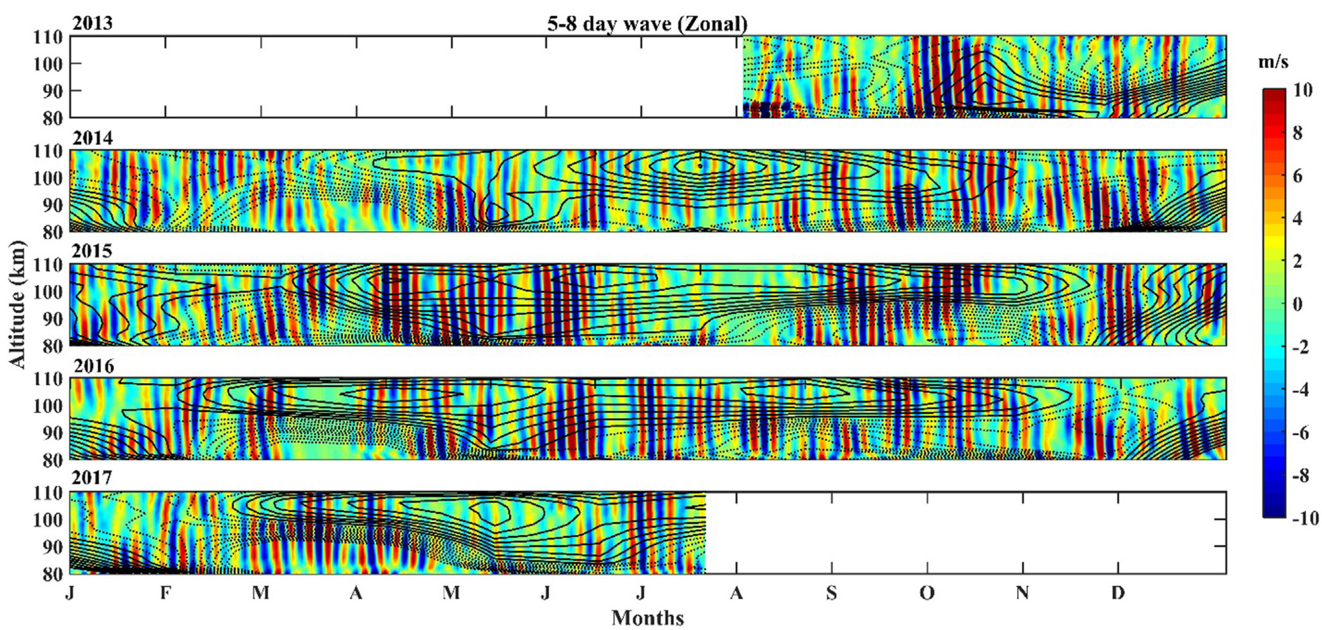

Fig. 10. Contours of 6.5 day band-pass filtered zonal wind superimposed with mean zonal wind from August 2013-July2017 for 80–110 km height.

are observed at higher altitude (above 90 km) during summer months and fall equinox of years 2015 and 2016, where the background mean wind is eastward. The eastward shearing is again observed during December solstice. A weak 6.5-day wave activity observed during the year 2017. A large inter-annual variability is observed in the 6.5-day wave activity.

The 6.5-day wave activity in meridional wind is less as compared with the zonal wind (shown in Fig. 11). A very less/ rare wave activity has been observed during the year 2017 as compared with remaining years. Similar to the zonal component, the wave activity in the meridional component is large near equinoxes and summer months when background wind is equatorward (southward). The burst like wave activity is observed at all altitudes during summer months and is predominantly at upper mesospheric altitudes (80–90 km) during equinoxes. The 6.5-day waves are interestingly observed during December solstice over all altitudes when background mean wind is poleward (northward). The observed results implicate a clear seasonal dependence of 6.5-day wave. (Meyer and Forbes 1997) reported that the middle atmospheric wind field during the equinoctial period is beneficial for the generation of wave field through instabilities. And in-situ momentum

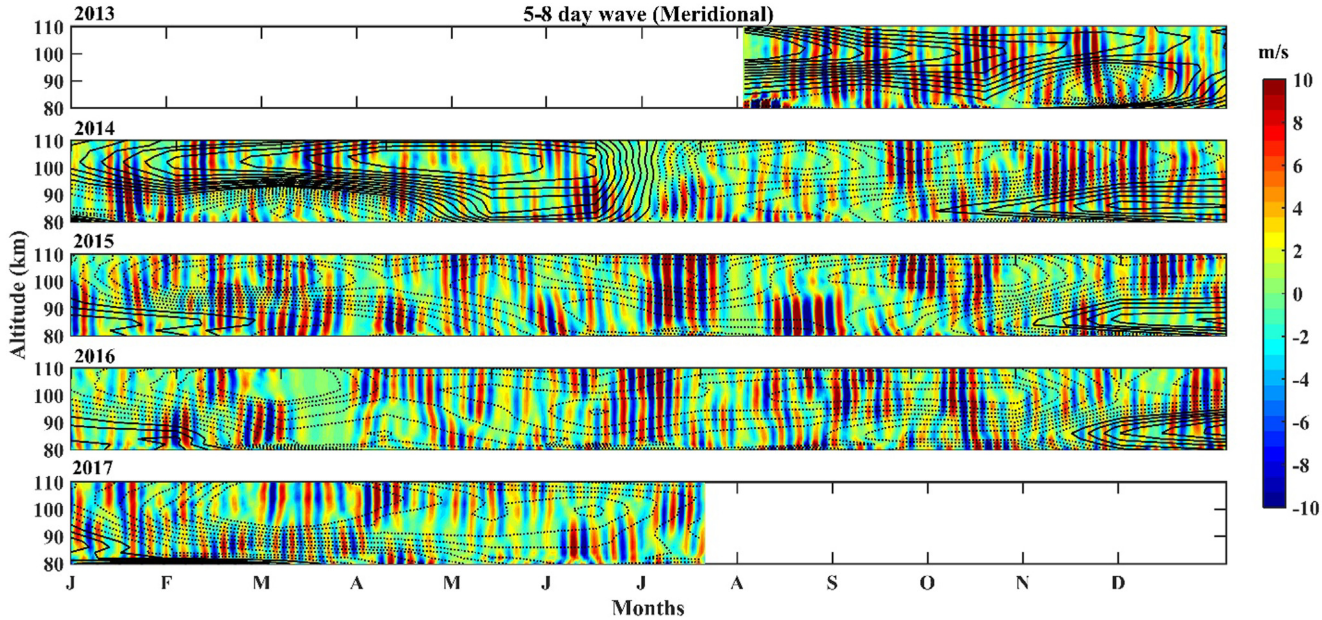

Fig. 11. Contours of 6.5 day band-pass filtered meridional wind superimposed with mean meridional wind from August 2013-July2017 for 80–110 km height.

forcing will be strongly responsible at high latitudes in the southern hemisphere. However, significant amplitude of this wave activity is observed even in the meridional wind using MLT radar at middle and high latitude (Clark et al. 2002); (Pogoreltsev et al. 2002).

3.2.2. Seasonal variation in 6.5-day wave

The seasonal variation in the 5–8 day wave is shown in the analysis of Fig. 12. In this figure, the contours shown are for 5–8 day wave amplitude. A 5–7 day zonal wave (Fig. 12(a)) is most common during the spring and fall equinoctial months. The 6.5-day wave amplitudes observed during the spring equinox are much larger than those of the fall equinoctial months. The wave amplitudes are stronger at higher altitudes than at lower ones, suggesting that the wave amplitudes increase with height. Above 84 km, the wave activity attains its maximum value. The wave amplitude reaches $\sim$ 8 m/s at altitudes of 86–100 km. Similar to SAO, the 6.5-day wave activity is stronger in April than in September, showing a possible effect of SAO on this wave. The middle atmospheric wind field during the equinoctial months is conducive for the generation, propagation and

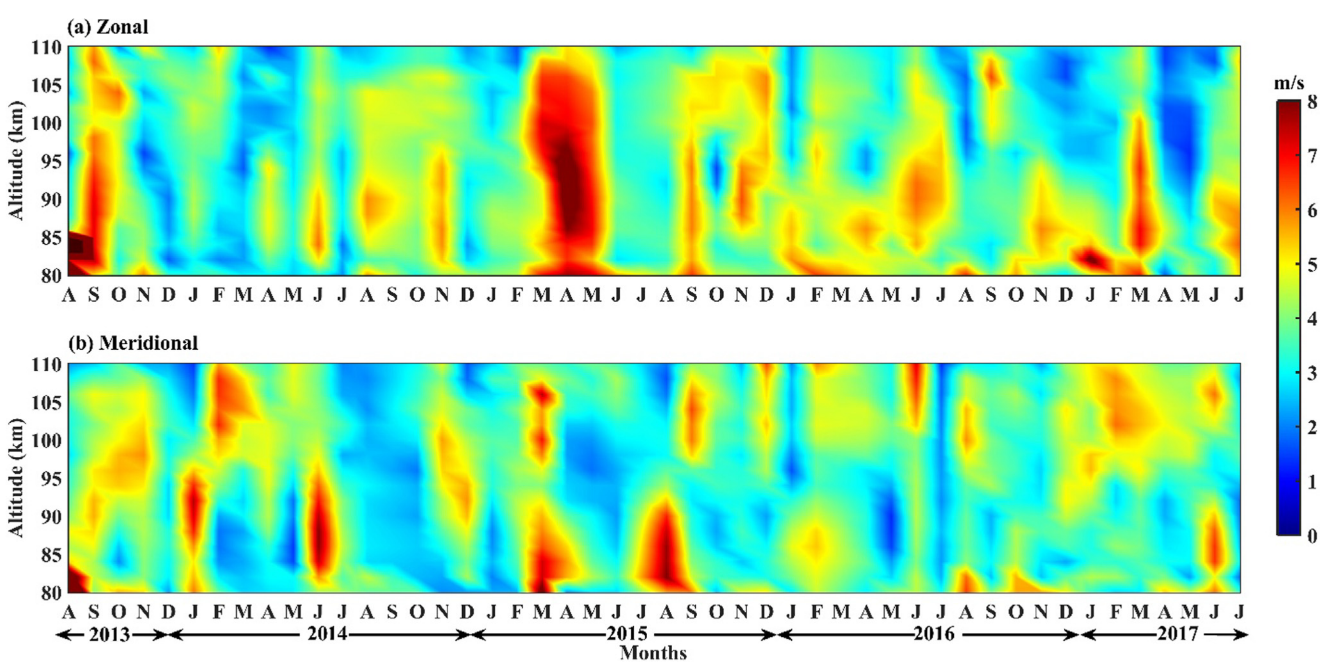

Fig. 12. Seasonal variation in (a) zonal and (b) meridional 5–8 day wave.

amplification of the wave by gaining energy from unstable regions. This is because the wind field is still relatively weak compared with solstice period so that the wave may propagate without much decay (Kishore et al., 2004; Liu et al., 2004; Meyer and Forbes, 1997). A large inter-annual variability is observed in the wave activity, which is stronger in the year 2015 than in the remaining two years (2014 and 2016). Also, moderate amplitudes are observed during the May and October months. In the month of May, the wave activity appears at mesospheric heights (below 92 km) where the zonal wind is westward. The wave activity in the meridional component (Fig. 12(b)) is observed to be strong during the solstices (June-July and December-February). Also, the wave activity was strong during the years 2014 and 2015. The meridional wave activity is strong in the MLT region but has slightly less amplitude as compared with the zonal component during 2016 and 2017. In general, the 6.5-day meridional wave activity is not consistent.

3.2.3. Amplitude and phase variation of 6.5- day wave

From the seasonal variation of the 6.5-day wave, it can be clearly seen that the largest bursts (amplitude greater than 7 m/s) occur during the 3 equinoxes (September 2013, April 2015, and March 2017). All the other equinox bursts look "normal" (Fig. 12). Therefore, here the harmonic analysis is done for the equinoctial period and presented in Fig. 13. The time series of the zonal component is the least square fitted for the 6.5-day harmonic component. The zonal amplitude during the spring equinox is generally less than 5 m/s in all years except 2015. The maximum amplitudes (3–6 m/s) are observed in the fall equinox at the 84–98 km altitude range, compared to that of the spring equinoctial period, and the reverse is the case for the year 2015. From Fig. 13, it is clear that during both the equinoxes (spring and fall), almost all the occurrences of the 6.5-day wave at the 84–98 km altitude range fall in the case when the zonal wind is easterly (westward).

3.3. 16-day oscillations

The 15–17 day oscillations are referred to as the 16-day oscillations. These oscillations in nature are supposed to have a global scale, and the westerly phase of the zonal background winds is more favorable for the 16-day wave penetration to the MLT region. Earlier observations have shown that this planetary-scale oscillation (16-day) exhibits year-to-year variability but does not show any seasonal behavior, either for Zonal or Meridional components [e.g. (Lima et al., 2006; Namboothiri et al., 2002)]. However, maximum wave activities were observed in the months January and February. During these months, the wave exists over a large part of the MLT region, with amplitudes generally decreasing with altitude. In particular, the waves can be seen up to the lower thermospheric (100 km) region. Also, the zonal component of the 16-day wave is larger in amplitude than the meridional component. The 16-day wave is extracted by using a band-pass filter with a pass-band between 15 and 17 days.

3.3.1. Time domain filtering

The contours of the 16-day filtered wave with mean winds superimposed of zonal and meridional winds are shown in Figs. 14 and 15 respectively. The 16-day zonal wave activity (Fig. 14) has been observed during December-February of every year when the background mean wind is eastward. In addition to this, wave activity is predominant over all seasons at all altitudes. The results observed with the Kolhapur radar are in good agreement with the results reported earlier by (Das et al., 2010;

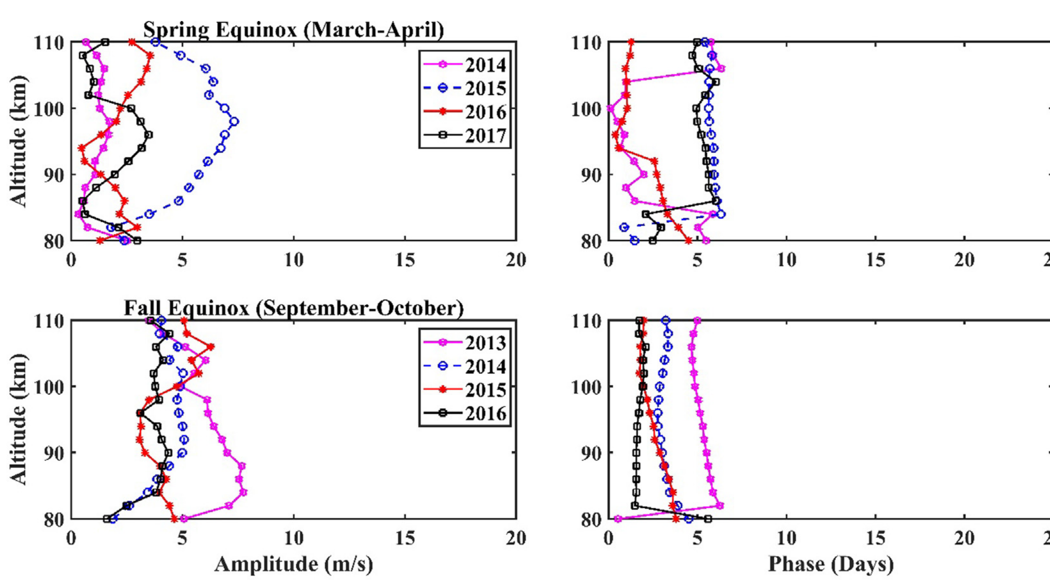

Fig. 13. Vertical profile of the 6.5- day wave amplitude (left panel) and phase (right panel) of zonal wind during spring (upper panel) and fall (lower panel) equinoxes.

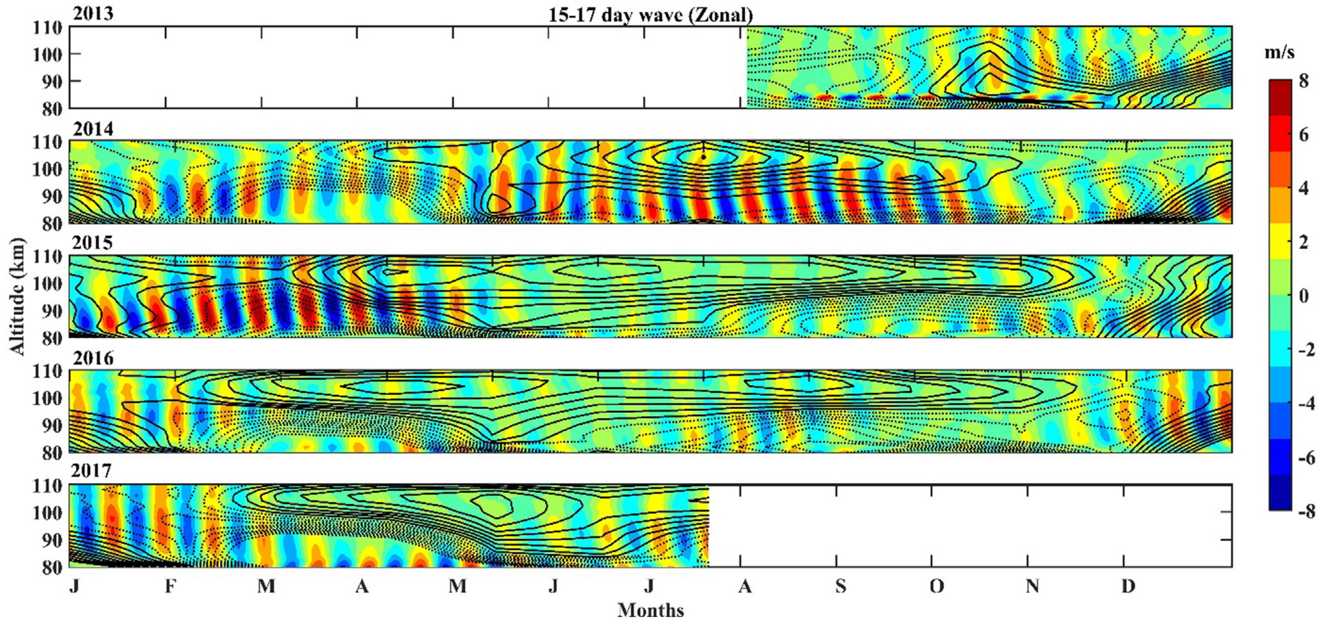

Fig. 14. Contours of 16-day band-pass filtered zonal wind superimposed with mean zonal wind from August 2013-July2017 for 80–110 km height.

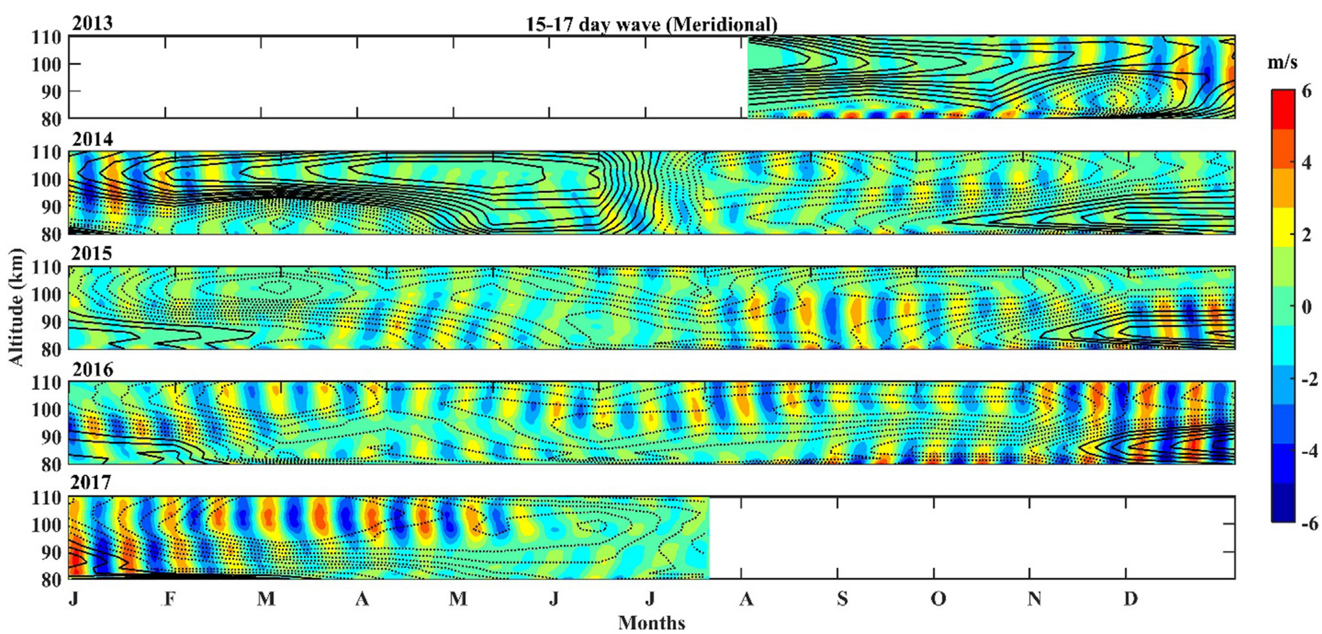

Fig. 15. Contours of 16 day band-pass filtered meridional wind superimposed with mean meridional wind from August 2013-July2017 for 80–110 km height.

Jiang et al., 2005; Luo et al., 2002; Namboothiri et al., 2002). They have reported that these waves no longer remain dominated in winter; instead, the waves spread to almost all seasons and altitudes of the MLT region at subtropical and equatorial locations.

The 16-day wave activity observed in the meridional component (Fig. 15) is present for the analyzed period, but the amplitude is small as compared with the zonal component. Similar to the zonal component, the 16-day wave is spread over all seasons at all altitudes. The 16-day waves are present with slightly high amplitude (~4 m/s) during the winter season when the background mean wind is poleward (Northward) at upper mesospheric heights (80–90 km).

3.3.2. Seasonal variation in 16- day planetary scale oscillation

The seasonal variation in the 16-day wave is shown in the analysis of Fig. 16. In this analysis, the monthly 16-day wave amplitude for both the wind components is calculated at every height (80–110 km). The zonal 16-day wave is visible in Fig. 16(a) during the months of January and

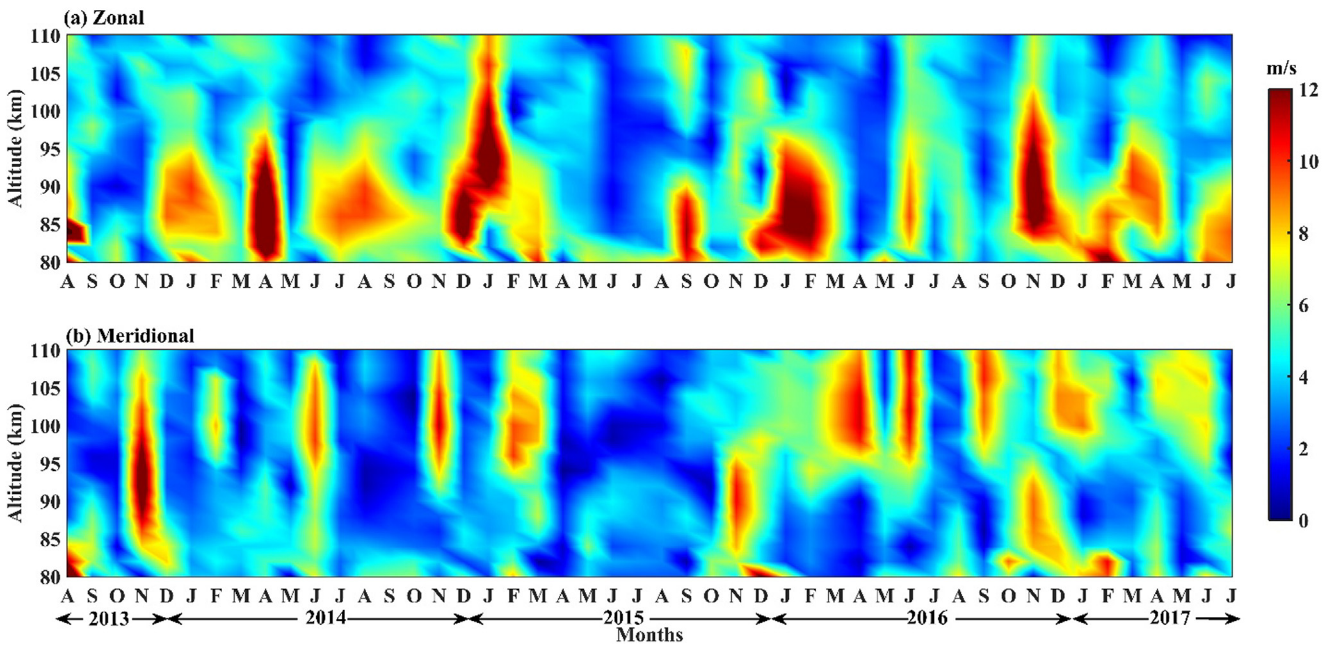

Fig. 16. Seasonal variation in (a) Zonal (b) Meridional 16- day wave.

February of each year of the analyzed period. In addition, the wave activity is also observed during the summer months of the year 2014, March–April of 2014 and 2017, September–October of 2015, and June–July of 2016 and 2017. In the meridional component (Fig. 16 (b)) of wind, the wave activity was observed during the winter months of every year but at higher altitudes except in 2013, 2015, and 2017. From the analysis of Fig. 16, it has been observed that no significant seasonal variation is seen in the 16-day wave.

3.3.3. Amplitude and phase variation of 16- day planetary scale oscillation

The amplitude and phase of 16-day planetary scale oscillations can be determined by harmonic analysis. The amplitude and phase of the zonal and meridional components of wind for the months of January and February are presented in the analysis of Fig. 17.

The peak 16-day zonal wave activity (upper panel) was observed during the year 2015 and the peak amplitude observed was 12 m/s at mesopause height. Whenever the

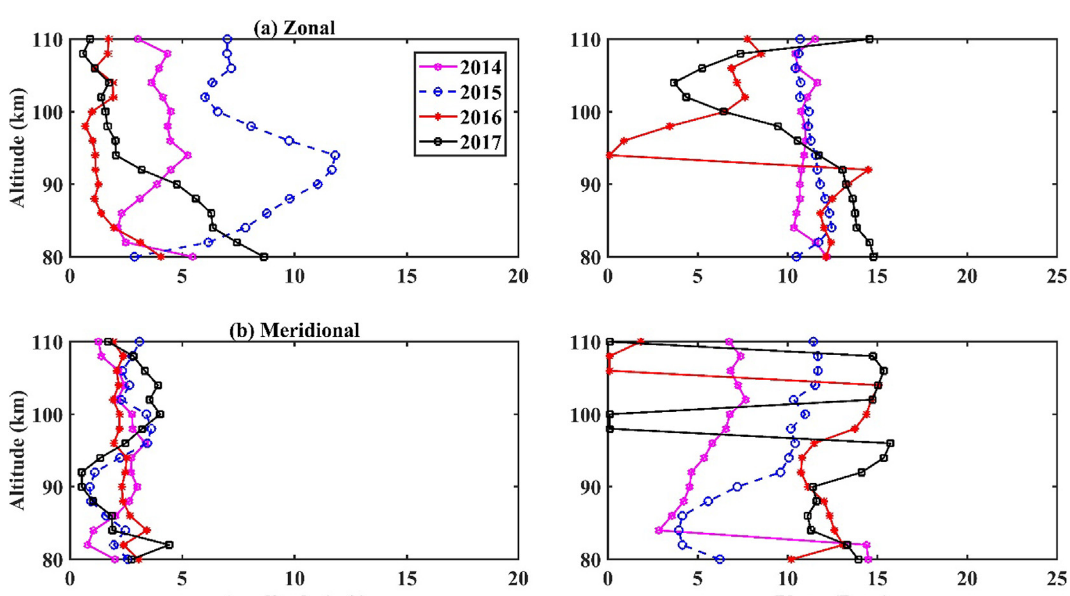

Fig. 17. Vertical profile of the 16- day wave amplitude (left panel) and phase (right panel) of (a) zonal (upper panel) and (b) meridional (lower panel) winds during the month of January-February.

wave amplitude is observed to be less, large phase variability is observed (2016 and 2017). Similar results were observed in the meridional component (lower panel), but the amplitude observed was smaller than the zonal component of wind. In addition to the large amplitude observed at upper mesospheric heights (80–86 km), the 16-day wave amplitude is also observed at lower thermospheric heights (90–104 km).

3.4. Madden-Julian oscillation (MJO)

3.4.1. Spectral analysis of MJO using FFT technique

The dominant period of MJO is roughly spread over a time period of 30–60 days (Fig. 2). Its peak power is highly variable within this range of period. The spectral amplitude of zonal and meridional winds is presented through the analysis of Fig. 2. From the analysis, the MJO is clearly observed in a zonal component within this range of period. From the analysis, it has been observed that the altitude occurrence of MJO is between 80 and 90 km. The MJO amplitude of meridional wind is negligibly weak.

3.4.2. Time domain filtering

The MJO variability in the band-pass (pass-band of 30 and 60 days) filtered zonal wind during the observation span has been presented through the analysis in Fig. 18 (a). The wave amplitude of MJO in the MLT region is quite high (~12 m/s) as compared with the others reported in this article. The MJOs are observed almost at all altitudes but more prominently at upper mesospheric heights (below 80–90 km). In general, the burst of zonal MJO is observed during the winter months at all altitudes (80–110 km), while in the summer months it occurs at higher altitudes (above 90 km). Normally during winter seasons long period oscillations like MJOs generated in the lower atmosphere will get dissipated in the mesopause region either due to convective or dynamic instabilities or due to critical filtering mechanism (Ramkumar et al. 2006). From the analysis, it is worth noting that the zonal MJO occurred when the background mean wind was eastward. Similar to the zonal component, the meridional MJOs (Fig. 18 (b)) are observed during the winter and summer months. The zonal wave amplitudes are observed to be larger during all winters while smaller during some of the summers (for example, 2016) than that of the meridional component.

3.4.3. Amplitude and phase variation of MJO

The vertical profiles of amplitude and phase variation of the zonal and meridional MJO are presented in Figs. 19 and 20. In the summer months, the zonal MJO (Fig. 19) amplitude is observed to be maximum at higher altitudes (above ~ 90 km), while during winter it is between 80 and 94 km. The amplitudes observed during the summer are larger as compared with the winter months. The phase of MJO is gradually decreased as height increases, except for the year 2016. During 2016, large phase variation was observed while the amplitude observed was very small in both the seasons. From this analysis, it can be seen that there is a large intraseasonal variability observed in the MLT Madden-Julian Oscillation.

Except for 2015 and 2016, a large amplitude (3 to 5 m/s) of MJO in the meridional component (Fig. 20) has been observed during the summer at all altitudes. During the winter season, the MJO amplitude is negligible at mesospheric heights (80–90 km) while considerably large (~2 to 3 m/s) at higher altitudes (above 90 km). The phase

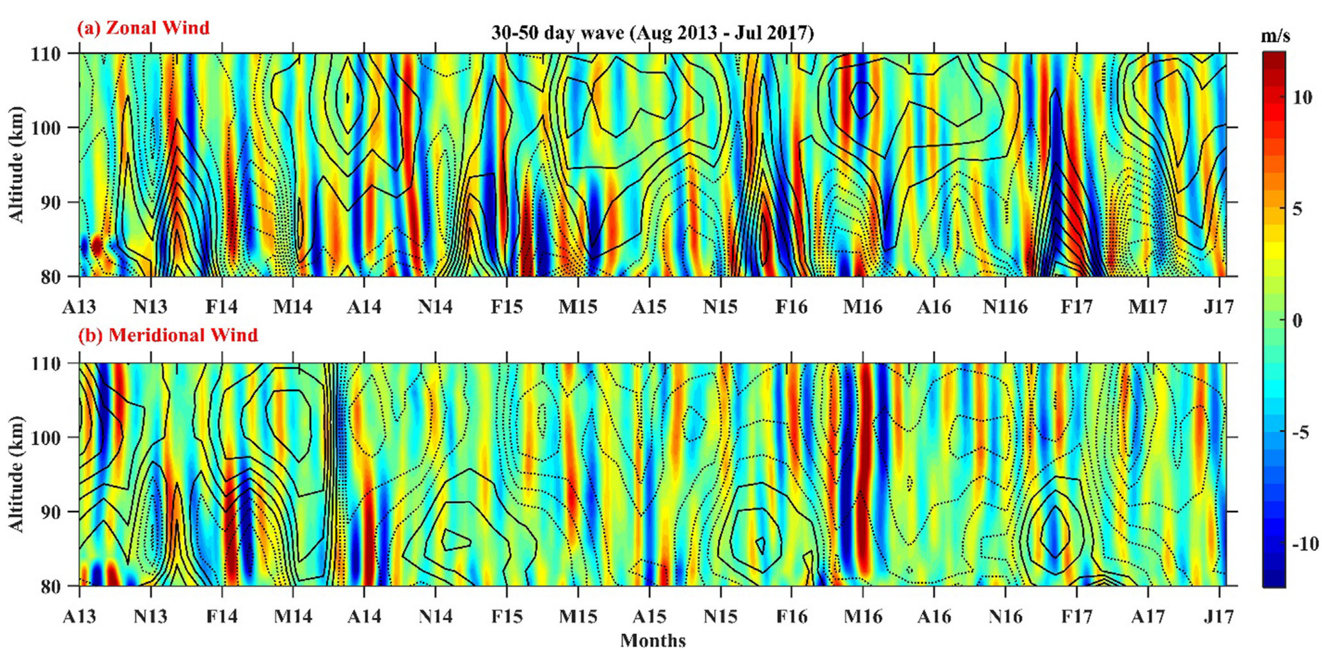

Fig. 18. Contours of band-pass filtered (cut offs 30 and 60 days) (a) zonal and (b) meridional wind with superimposed mean zonal and meridional wind respectively.

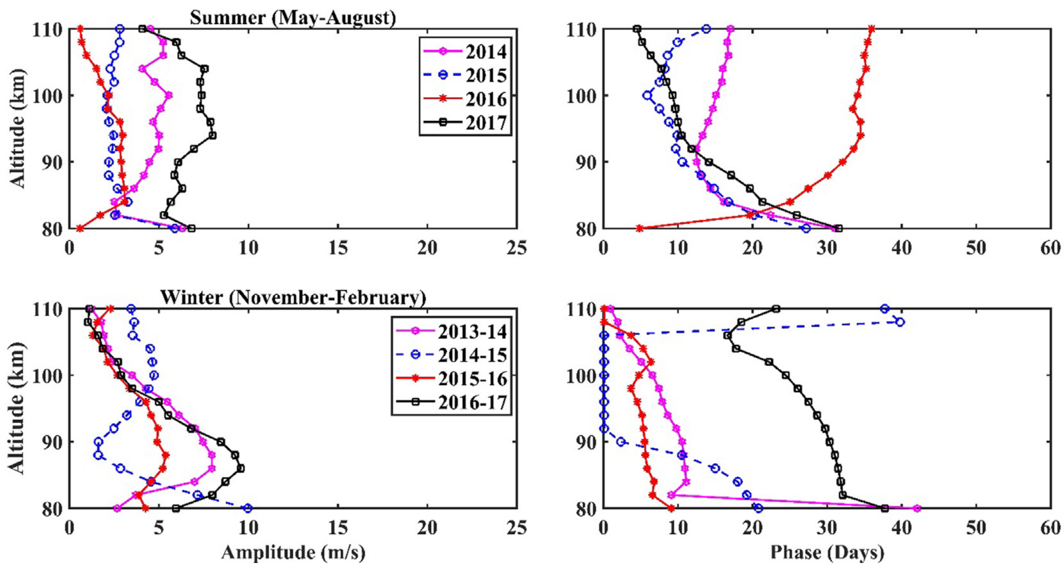

Fig. 19. Vertical profile of the MJO amplitude (left panel) and phase (right panel) of zonal wind during the summer (upper panel) and winter months (lower panel).

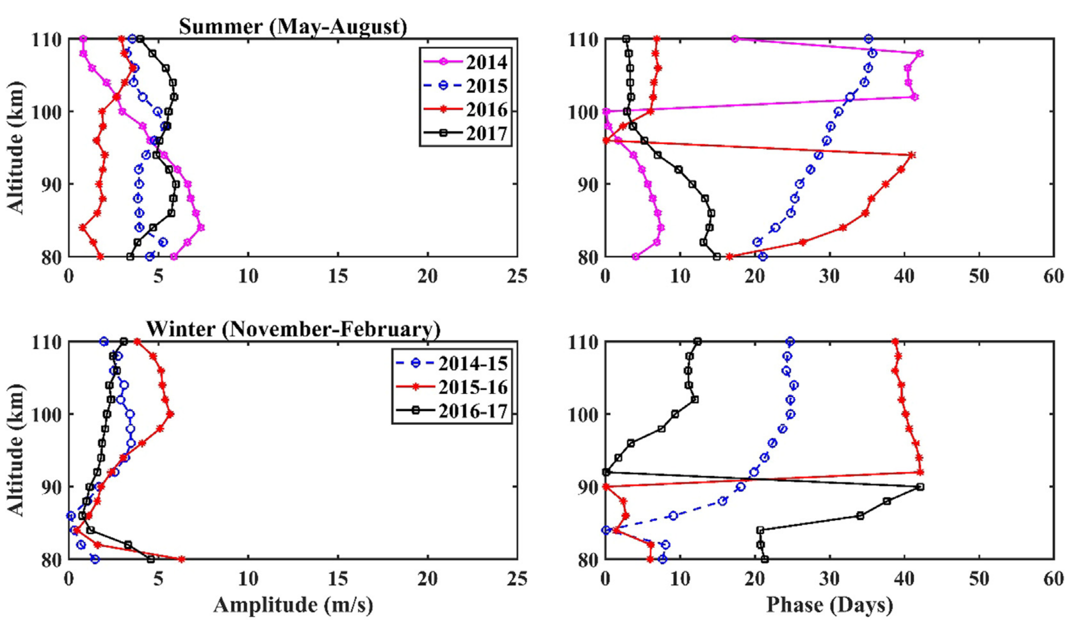

Fig. 20. Vertical profile of the MJO amplitude (left panel) and phase (right panel) of meridional wind during the summer (upper panel) and winter months (lower panel).

gradually decreases as height increases, except for the years 2015 summer and 2014–2015 winter. Also, large phase variation is observed when the amplitude is small. Similar to the zonal component, large intraseasonal variability is observed in the meridional MJO.

4. Discussion and conclusions

We provide the analysis of MF radar at the low latitude station, Kolhapur. From our analysis we infer that the UFK wave is stronger in the spring equinoctial period, i.e., the first westward phase of the SAO of zonal wind. The UFK waves reveal semiannual variability at heights $\sim$ 85 km. At these heights, mesopause semiannual oscillations (MSAO) in the zonal wind peaks. As suggested by (Yoshida et al. 1999), this variability is caused by the interaction of the wave with the mean wind in the underlying stratopause semiannual oscillation (SSAO) regime. The amplitude of the UFK wave is observed to be larger when the mean winds blow westward and is observed up to the highest altitude of 100 km. The 6.5-day wave is observed to be an equinoctial phenomenon, being strong during the months of April/May and September/October, when the background winds are westward. Similar to SAO, the wave activity is stronger in April/May than in September/October. This indicates the influence of SAO on this wave.

The 16-day zonal wave has a larger amplitude than that of the meridional component. The 16-day waves penetrate into the MLT region along the lines of a weak background eastward wind. The eastward motion of the zonal background winds is favorable for these waves to penetrate. The strong summer waves during 2014 may come from the winter in the southern hemisphere. For this, large and multi-station data sets are needed for the analysis. Both the wind components, i.e., zonal and meridional winds, do not exhibit any seasonal characteristics (ex. SAO) of a 16-day planetary wave.

MJO is observed when the background wind is eastward with an average speed of $\sim$ 5 m/s, which occurs during the summer and winter months. This is one of the most fundamental differences between MJO and other tropical atmosphere phenomena such as convectively coupled Kelvin waves, which propagate eastward at speeds of 15–17 m/s (e.g., (Wheeler and Kiladis 1999); (Straub and Kiladis 2002)). A large intraseasonal variability has been observed in both the zonal and meridional components of winds.

Declaration of Competing Interest

The authors declare that they have no known competing financial interests or personal relationships that could have appeared to influence the work reported in this paper.

Acknowledgement

One of the authors (Dr. H. P. Gaikwad) is thankful to Dr. M. V. Ratnam, Scientist ‘F’, NARL, Gadanki for his consistence guidance and support throughout the work.

References

Briggs, B.H., 1977. Ionospheric drifts. J. Atmos. Terr. Phys. 39, 1023–1033. https://doi.org/10.1016/0021-9169(77)90011-3.

Clark, R.R., Burrage, M.D., Franke, S.J., Manson, a. H., Meek, C.E., Mitchell, N.J., Muller, H.G., 2002. Observations of 7-d planetary waves with MLT radars and the UARS-HRDI instrument. Journal of Atmospheric and Solar-Terrestrial Physics 64, 1217–1228. https://doi.org/10.1016/S1364-6826(02)00070-6

Das, S.S., Kumar, K.K., Veena, S.B., Ramkumar, G., 2010. Simultaneous observation of quasi 16 day wave in the mesospheric winds and temperature over low latitudes with the SKiYMET radar. Radio Sci. 45, 1–11. https://doi.org/10.1029/2009RS004300.

Dhanya, R., Gurubaran, S., Emperumal, K., 2008. Lower E-region echoes over the magnetic equator as observed by the MF radar at Tirunelveli (8.7° N, 77.8° E) and their relationship to Esq and Esb. Ann. Geophys. 26, 2459–2470. https://doi.org/10.5194/angeo-26-2459-2008.

Forbes, J.M., Hagan, M.E., Miyahara, S., Vial, F., Manson, A.H., Meek, C.E., Portnyagin, Y.I., 1995. Quasi 16-day oscillation in the mesosphere and lower thermosphere. J. Geophys. Res. 100, 9149. https://doi.org/10.1029/94JD02157.

Gaikwad, H.P., Sharma, A.K., Gurav, O.B., Chavan, G.A., Nade, D.P., Patil, P.T., Nikte, S.S., Naniwadekar, G.P., 2019. Seasonal, annual, and interannual variability in MLT quasi-two-day waves over the low-latitude region Kolhapur (16.8°N; 74.2°E). Adv. Space Res. 63, 2100–2117. https://doi.org/10.1016/j.asr.2018.12.029.

Garcia, R.R., Lieberman, R., Russell, J.M., Mlynczak, M.G., 2005. Large-scale waves in the mesosphere and lower thermosphere observed by SABER. J. Atmos. Sci. 62, 4384–4399. https://doi.org/10.1175/JAS3612.1.

Guharay, A., Pant, P., Pande, B., Pandey, K., 2011. Observations of the ultra-fast Kelvin wave in the tropical mesosphere during equinox. Int. J. Remote Sens. 32, 3043–3053. https://doi.org/10.1080/01431161.2010.541522.

Gurubaran, S., Dhanya, R., Sathishkumar, S., Paramasivan, B., 2007. On the electric field control of the MF radar scatterers in the lower E region over the magnetic equator. Geophys. Res. Lett. 34. https://doi.org/10.1029/2006GL028748.

Gurubaran, S., Rajaram, R., 2000. Signatures of equatorial electrojet in the mesospheric partial reflection drifts over magnetic equator. Geophys. Res. Lett. 27, 943–946. https://doi.org/10.1029/1999GL003733.

Hirota, I., 1978. Equatorial waves in the upper stratosphere and mesosphere in relation to the semiannual oscillation of the zonal wind. J. Atmos. Sci. https://doi.org/10.1175/1520-0469(1978)035<0714:EWITUS>2.0.CO;2.

Hitchman, H.M., Leovy, C.B., 1988. Estimation of the Kelvin wave contribution to the semiannual oscillation. J. Atmos. Sci. 45, 1462–1475.

Holton, J.R., Lindzen, R.S., 1972. An updated theory for the quasi-biennial cycle of the tropical stratosphere. J. Atmos. Sci. https://doi.org/10.1175/1520-0469(1972)029<1076:AUTFTQ>2.0.CO;2.

Jiang, G.Y., Xiong, J.G., Wan, W.X., Ning, B.Q., Liu, L.B., Vincent, R. A., Reid, I., 2005. The 16-day waves in the mesosphere and lower thermosphere over Wuhan (30.6°N, 114.5°E) and Adelaide (35°S, 138°E). Adv. Space Res. 35, 2005–2010. https://doi.org/10.1016/j.asr.2005.03.011.

Jiang, G., Xu, J., Xiong, J., Ma, R., Ning, B., Murayama, Y., Thorsen, D., Gurubaran, S., Vincent, R. a., Reid, I., Franke, S.J., 2008. A case study of the mesospheric 6.5-day wave observed by radar systems. Journal of Geophysical Research: Atmospheres 113, 1–12. https://doi.org/10.1029/2008JD009907

Kishore, P., Namboothiri, S.P., Igarashi, K., Gurubaran, S., Sridharan, S., Rajaram, R., Venkat Ratnam, M., 2004. MF radar observations of 6.5-day wave in the equatorial mesosphere and lower thermosphere. J. Atmos. Sol. Terr. Phys. 66, 507–515. https://doi.org/10.1016/j.jastp.2004.01.026.

Lieberman, R.S., Riggin, D., 1997. High resolution Doppler imager observations of Kelvin waves in the equatorial mesosphere and lower thermosphere. J. Geophys. Res. 102, 26117–26130. https://doi.org/10.1029/96JD02902.

Lima, L.M., Batista, P.P., Clemesha, B.R., Takahashi, H., 2006. 16-day wave observed in the meteor winds at low latitudes in the southern hemisphere. Adv. Space Res. 38, 2615–2620. https://doi.org/10.1016/j.asr.2006.03.033.

Liu, H.L., Talaat, E.R., Roble, R.G., Lieberman, R.S., Riggin, D.M., Yee, J.H., 2004. The 6.5-day wave and its seasonal variability in the middle and upper atmosphere. J. Geophys. Res. D: Atmos. 109, 1–13. https://doi.org/10.1029/2004JD004795.

Luo, Y., Manson, A.H., Meek, C.E., Meyer, K., Forbes, M., 2000. The quasi 16-day oscillations in the mesosphere and lower thermosphere at Saskatoon (52øN, 107øW), 1980–1996. J. Geophys. Res. 105, 2125–2138.

Luo, Y., Manson, A.H., Meek, C.E., Igarashi, K., Jacobi, C., 2001. Extra long period (20 – 40 day) oscillations in the mesospheric and lower thermospheric winds : observations in Canada , Europe and Japan , and considerations of possible solar in uences 63, 835–852

Luo, Y., Manson, a. H., Meek, C.E., Meyer, C.K., Burrage, M.D., Fritts, D.C., Hall, C.M., Hocking, W.K., MacDougall, J., Riggin, D.M., Vincent, R. a., 2002. The 16-day planetary waves: multi-MF radar observations from the arctic to equator and comparisons with the HRDI measurements and the GSWM modelling results. Annales Geophysicae 20, 691–709. https://doi.org/10.5194/angeo-20-691-2002

Matsuno, T., 1966. Quasi-geostrophic motions in the equatorial area. J. Meteorol. Soc. Japan. Ser. II 44, 25–43. https://doi.org/10.2151/jmsj1965.44.1_25.

Meyer, C.K., Forbes, J.M., 1997. A 6.5-day westward propagating planetary wave: origin and characteristics. J. Geophys. Res. 102, 26173. https://doi.org/10.1029/97JD01464.

Namboothiri, S.P., Kishore, P., Igarashi, K., 2002. Climatological studies of the quasi 16-day oscillations in the mesosphere and lower thermosphere at Yamagawa (31.2° N, 130.6° E), Japan. Ann. Geophys. 20, 1239–1246. https://doi.org/10.5194/angeo-20-1239-2002.

Pancheva, D., Mukhtarov, P., 2000. Wavelet analysis on transient behaviour of tidal amplitude fluctuations observed by meteor radar in the lower thermosphere above Bulgaria. Ann. Geophys. 18, 316–331. https://doi.org/10.1007/s00585-000-0316-3.

Pancheva, D., Mukhtarov, P., Siskind, D.E., Smith, A.K., 2016. Global distribution and variability of quasi 2 day waves based on the NOGAPS-ALPHA reanalysis model. J. Geophys. Res. Space Phys. 121, 11422–11449. https://doi.org/10.1002/2016JA023381.

Pogoreltsev, A.I., Fedulina, I.N., Mitchell, N.J., Muller, H.G., Luo, Y., Meek, C.E., Manson, A.H., 2002. Global free oscillations of the atmosphere and secondary planetary waves in the mesosphere and lower thermosphere region during August/September time conditions. J. Geophys. Res. Atmos. 107, 1–12. https://doi.org/10.1029/2001JD001535.

Ramkumar, T.K., Gurubaran, S., Rajaram, R., 2002. Lower E-region MF radar spaced antenna measurements over magnetic equator. J. Atmos. Sol. Terr. Phys.

Ramkumar, T.K., Bhavanikumar, Y., Rao, D.N., Gurubaran, S., 2006. Observational evidences on the influences of tropical lower atmospheric $ 20 day oscillation on the ionospheric equatorial electrojet. J. Atmos. Sol. Terr. Phys. 68, 523–538. https://doi.org/10.1016/j.jastp.2005.03.026.

Reddi, C.R., Ramkumar, G., 1995. Long period wind oscillations in the meteor region over Trivandrum (8 N, 77E). J. Atmos. Sol. Terr. Phys. 57.

Reed, R.J., 1964. A tentative model of the 26???month oscillation in tropical latitudes. Q. J. R. Meteorolog. Soc. 90, 441–466. https://doi.org/10.1002/qj.49709038607.

Reed, R.J., Wolfe, J.L., Nishimoto, H., 1963. A Spectral Analysis of the Energetics of the Stratospheric Sudden Warming of Early 1957. J. Atmos. Sci.

Reed, R.J., 1965. The Quasi-Biennial Oscillation of the Atmosphere Between 30 and 50 km Over Ascension Island.

Reid, I.M., 2015. MF and HF radar techniques for investigating the dynamics and structure of the 50 to 110 km height region : a review. In: Progress in Earth and Planetary Science. Progress in Earth and Planetary Science. https://doi.org/10.1186/s40645-015-0060-7.

Salby, M.L., Hartmann, D.L., Bailey, P.L., Gille, J.C., 1984. Evidence for equatorial Kelvin modes in Nimbus-7 LIMS. J. Atmos. Sci. https://doi.org/10.1175/1520-0469(1984)041<0220:EFEKMI>2.0.CO;2.

Salby M., L., 1981. Rossby Normal Modes in Nonuniform Background Configurations, Part I: Simple Fields 38.

Shankar, S., 2012. Characteristics of the Quasi-16 day wave in the mesosphere and lower thermosphere (MLT): a review over an equatorial station Thumba (8.5oN, 76.5oE). Modern Climatol. https://doi.org/10.5772/33641.

Sharma, A.K., Gaikwad, H.P., Ratnam, M.V., Gurav, O.B., Ramanjaneyulu, L., Chavan, G.A., Sathishkumar, S., 2018. Diurnal, monthly and seasonal variation of mean winds in the MLT region observed over Kolhapur using MF radar. J. Atmos. Sol. Terr. Phys. https://doi.org/10.1016/j.jastp.2018.01.028.

Sridharan, S., Gurubaran, S., Rajaram, R., 2002. Radar observations of the 3.5-day ultra-fast Kelvin wave in the low-latitude mesopause region, Journal of Atmospheric and Solar-Terrestrial Physics.

Straub, K.H., Kiladis, G.N., 2002. Observations of a convectively coupled Kelvin wave in the Eastern Pacific ITCZ. J. Atmos. Sci. 59, 30–53. https://doi.org/10.1175/1520-0469(2002)059<0030:OOACCK>2.0.CO;2.

Takahashi, H., Wrasse, C.M., Pancheva, D., Abdu, M.A., Batista, I.S., Batista, P.P., Clemesha, B.R., Shiokawa, K., Takahashi, H., Wrasse, C.M., Pancheva, D., Abdu, M.A., Batista, I.S., 2006. Signatures of 3 ? 6 day planetary waves in the equatorial mesosphere and ionosphere To cite this version : Annales Geophysicae Signatures of 3 – 6 day planetary waves in the equatorial mesosphere and ionosphere.

Takahashi, H., Wrasse, C.M., Fechine, J., Pancheva, D., Abdu, M.A., Batista, I.S., Lima, L.M., Batista, P.P., Clemensha, B.R., Schuch, N.J., Shiokawa, K., Gobbi, D., Mlynczak, M.G., Russell, J.M., 2007. Signatures of ultra fas Kelvin waves in the equatorial middle atmosphere and ionosphere. Geophys. Res. Lett. 34, 2–7. https://doi.org/10.1029/2007GL029612.

Talaat, E.R., Yee, J.-H., Zhu, X., 2001. Observations of the 6.5-day wave in the mesosphere and lower thermosphere. J. Geophys. Res.: Atmos. 106, 20715–20723. https://doi.org/10.1029/2001JD900227.

Talaat, E., Yee, J., 2002. The 6.5-day wave in the tropical stratosphere and mesosphere. J. Geophys. Res. 107, 1–5. https://doi.org/10.1029/2001JD000822.

Torrence, C., Compo, G.P., 1998. A practical guide to wavelet analysis. Bull. Am. Meteor. Soc. 79, 61–78. https://doi.org/10.1175/1520-0477(1998)079<0061:APGTWA>2.0.CO;2.

Vincent, R.A., 1984. MF/HF radar measurements of the dynamics of the mesopause region—a review. J. Atmos. Terr. Phys. 46, 961–974. https://doi.org/10.1016/0021-9169(84)90003-5.

Vincent, R.A., Kovalam, S., Fritts, D.C., Isler, J.R., 1998. Long-term MF radar observations of solar tides in the low-latitude mesosphere: Interannual variability and comparisons with the GSWM. J. Geophys. Res. 103, 8667. https://doi.org/10.1029/98JD00482.

Vincent, R., Lesicar, D., 1991. Dynamics of the equatorial mesosphere: first results with a new generation partial reflection radar. Geophys. RF_Search Lett. 18, 825–828.

Wallace, J.M., Kousky, V.E., 1968. Observational evidence of kelvin waves in the tropical stratosphere. J. Atmos. Sci. https://doi.org/10.1175/1520-0469(1968)025<0900:OEOKWI>2.0.CO;2.

Wheeler, M., Kiladis, G.N., 1999. Convectively coupled equatorial waves: analysis of clouds and temperature in the wavenumber-frequency domain. J. Atmos. Sci. 56, 374–399. https://doi.org/10.1175/1520-0469(1999)056<0374:CCEWAO>2.0.CO;2.

Yee, J.H., Talaat, E.R., Zhu, X., 2001. 6.5 day planetary waves in the mesosphere and lower thermosphere. Adv. Space Res. 27, 1761–1765. https://doi.org/10.1016/S0273-1177(01)00331-3.

Yoshida, S., Tsuda, T., Shimizu, A., Nakamura, T., 1999. Seasonal variations of 3.0∼3.8-day ultra-fast Kelvin waves observed with a meteor wind radar and radiosonde in Indonesia. Earth Planets Space, 675–684.

Zhang, C., 2005. Madden-Julian oscillation. Rev. Geophys. 43, 1–36. https://doi.org/10.1029/2004RG000158.1.INTRODUCTION.